Quaternary Research **57**, 343–354 (2002)
doi:10.1006/qres.2002.2324, available online at http://www.idealibrary.com on IDEAL®

A Late Glacial–Holocene Tephrochronology for Glacial Lakes in Southern Ecuador

Donald T. Rodbell,[1] Stefan Bagnato,[2] and Jeffrey C. Nebolini[3]

Geology Department Union College, Schenectady, New York 12308-2311

Geoffrey O. Seltzer

Department of Earth Sciences, Syracuse University, Syracuse, New York 13244-1070

and

Mark B. Abbott[4]

Department of Geosciences, University of Massachusetts, Amherst, Massachusetts 01003-5820

Received June 26, 2001; published online April 23, 2002

Despite the presence of numerous active volcanoes in the northern half of Ecuador, few, if any, distal tephras have been previously recognized in the southern one third of the country. In this article, we document the presence of thin (0.1–1.0-cm-thick) distal tephras comprising glass and/or phenocrysts of hornblende and feldspar in sediment cores from five glacial lakes and one bog in Las Cajas National Park (2°40′–3°00′S, 79°00′–79°25′W). The lake cores contain from 5 to 7 tephras, and each has a diagnostic major element geochemistry as determined from electron microprobe analysis of ~710 glass shards and ~440 phenocrysts of feldspar and hornblende. The loss of sodium with exposure to the electron microbeam causes a 10 ± 7 wt.% ($\pm 1\sigma$) reduction in Na content, which we empirically determined and corrected for before correlating tephras among the sediment cores. We use a similarity coefficient to correlate among the sediment cores; pair-wise comparison of all tephras generally yields an unambiguous correlation among the cores. Six tephras can be traced among all or most of the cores, and several tephras are present in only one or two of the cores. Twenty-six accelerator mass spectrometry ^{14}C dates on macrofossils preserved in the sediment cores provide the basis for establishing a regional tephrochronology. The widespread tephras were deposited ~9900, 8800, 7300, 5300, 2500, and 2200 cal yr B.P. The oldest tephras were deposited ~15,500 and 15,100 cal yr B.P., but these are not found in all cores. Two of the tephras appear correlative with volcaniclastic strata on the flanks of Volcán Cotopaxi and one tephra may correlate with strata on the flanks of Volcán Ninahuilca; both volcanoes are in central Ecuador. The absence of tephras in sediment cores correlative with the numerous eruptions of active volcanoes of the past two millennia implies that the earlier eruptions, which did deposit tephras in the lakes, must have been either especially voluminous, or southerly winds must have prevailed at the time of the eruption, or both.

Key Words: **tephrochronology; South America; glacial lakes; Ecuador.**

INTRODUCTION

The spectacular stratovolcanoes of central Ecuador define the northern limit of a significant gap in the distribution of active volcanism that extends southward to southern Peru (Barazangi and Isacks, 1976). The northward transition to active (Holocene) volcanism occurs at Volcán Sangay (5230 m above sea level [asl], ~2°S; Fig. 1), which marks a major transition in the angle of subduction of the Nazca plate beneath western South America and in the thickness of the continental crust (Sillitoe, 1974; Barazangi and Isacks, 1976; Hall and Wood, 1985).

The numerous, active volcanoes northward of 2°S have generated enormous volumes of tephra, which dominate late Quaternary deposits of the region. On the most active volcanoes, such as Volcán Cotopaxi (5897 m asl), virtually all glacial landforms have been buried or obliterated by thick proximal tephras and/or pyroclastic-flow deposits. In regions surrounding these volcanoes, the landscape is mantled by thick (tens of meters) deposits of a loess-like mixture of fine-grained tephra and organic matter that commonly possess multiple paleosols. This latter is known locally as *cangagua* (Clapperton and Vera, 1986). The stratigraphy of volcaniclastic sediments in northern Ecuador has been reported by Mothes and Hall (1991), Mothes (1992), Hall and Beate (1991), and Hall and Mothes (1994), who have developed

[1] To whom correspondence should be addressed. E-mail: rodbelld@union.edu.

[2] Present address: Department of Earth and Atmospheric Sciences, ES 351-University at Albany, Albany, NY 12222.

[3] Present address: 285 Vly Road, Schenectady, NY 12309.

[4] Present address: Department of Geology and Planetary Science 321 Engineering Hall, University of Pittsburgh, Pittsburgh, PA 15260-3332.

0033-5825/02 $35.00

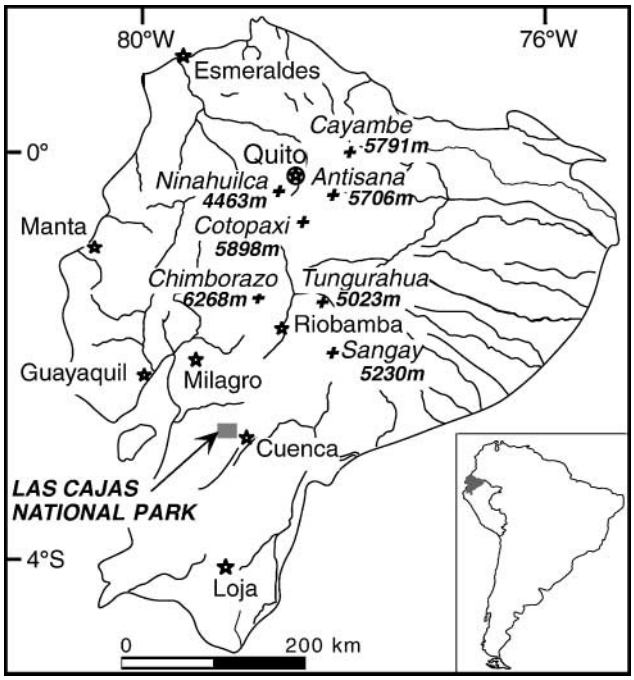

FIG. 1. Location of Las Cajas National Park in southern Ecuador. Names in italics are principal volcanoes or are mentioned in text; elevations are in meters.

an eruption chronology for the active volcanoes in central and northern Ecuador based on historical accounts and radiocarbon dating.

In contrast to the widespread *cangagua* and tephra of the northern two thirds of Ecuador, no such material has been reported from southern Ecuador. Here we report the first such evidence in the form of thin (~0.1 to 1.0-cm-thick) distal tephras deposited in glacial lakes and peat lands in Las Cajas National Park (Fig. 1).

The objectives of this study are to determine the geochemical fingerprint of tephras preserved in lakes in Las Cajas National Park, southern Ecuador, and to date these tephras by closely bracketing radiocarbon dates. We anticipate that the resultant tephrochronology will provide important isochrons for future paleolimnologic, geomorphic, and geoarcheologic studies in the region.

STUDY AREA

Las Cajas National Park (2°40′–3°00′S, 79°00′–79°25′W) straddles the continental divide in the southern Ecuadorian Andes approximately 25 km west of Cuenca and 300 km south–southwest of Quito (Figs. 1 and 2). The Park ranges in elevation from ~3100 to 4500 m asl and contains hundreds of glacial lakes (Fig. 2). The Park comprises a ~4000-m-high plateau and several deep valleys that drain to the west and east (Fig. 2). Bedrock is primarily thick Quaternary silicic ignimbrite, rhyolite, and andesite of the Tarqui Formation; also present are Cretaceous andesites of the Celica Formation and diorite intrusions, but these comprise less than 10% of the bedrock of the Park (Dirección General de Geología y Minas, 1975). Vegetation above 3000 m asl is humid páramo, which is characterized by tussock grasses and isolated "islands" of Andean forest; in the lower reaches of the Park, Andean forest is continuous. Mean annual precipitation (MAP) in Cuenca (2500 m asl; Fig. 1) is 880 cm yr^{-1}; MAP in the Park is undoubtedly higher and may exceed 2000 cm yr^{-1} at the higher elevations.

The region above ~2800 m asl was covered by a ~400-km^2 ice cap during the last local glacial maximum, and this was the most extensive late Quaternary glaciation. Radiocarbon dates from the base of high-elevation lakes and bogs indicate that the plateau was nearly ice free by ~12,000 ^{14}C yr B.P. (Rodbell *et al*., 1996). Although we have no firm radiometric age control for the maximum extent of late Quaternary glaciation, soil catena studies on moraines in the Tomebamba drainage (Fig. 2) suggest that all moraines are young and were probably deposited during marine isotope stage 2 (Goodman, 1996).

METHODS

Sediment cores 4.4–9.2 m in length from five lakes and one peatland (Fig. 2) were obtained with a square-rod piston corer (Wright, 1991) from an inflatable rubber raft. Lake water depths ranged from 8 to 14 m. Cores were taken in 1-m-long, nonoverlapping drives. All cores were extruded and described in the field, wrapped in plastic, and returned to the laboratory in PVC tubes.

Several techniques were employed to locate tephra layers within the sediment cores. Most layers can simply be distinguished by their color. Inasmuch as the Holocene section of most cores is a dark gyttja with 15–20 wt.% organic C, the light-gray tephras are distinct. However, some cores contain a complex sequence of thin laminae of gyttja alternating with light-colored inorganic clastic sediment, such as the core from Laguna Pallcacocha (Rodbell *et al*., 1999). In these cases, tephras were identified through the inspection of smear slides and confirmation of the presence of angular and vesicular glass shards and phenocrysts. Additionally, most tephra layers are coarser grained than the surrounding sediment, and the presence of tephra can be determined by gently scraping the core with a knife; tephra tend to be gritty, unlike the organic-rich lake sediments. Whole core magnetic susceptibility (MS) analysis can also be used to locate tephra layers due to the comparatively high MS of many tephras (Bagnato, 2000).

Samples of each tephra were then treated with up to 30 ml of 30% H_2O_2 to remove organic matter, sonicated, and then sieved through a 75-μm sieve. Only the >75–μm fraction of the tephras was analyzed. These grains were examined under a binocular microscope and approximately 100 grains were selected for analysis. Glass shards and phenocrysts were placed in a drop of thin-section epoxy on a petrographic slide. The grain mounts were then polished to a flat, smooth surface using 9-, 3-, and 1-μm diamond pastes followed by a 0.3-μm aluminum

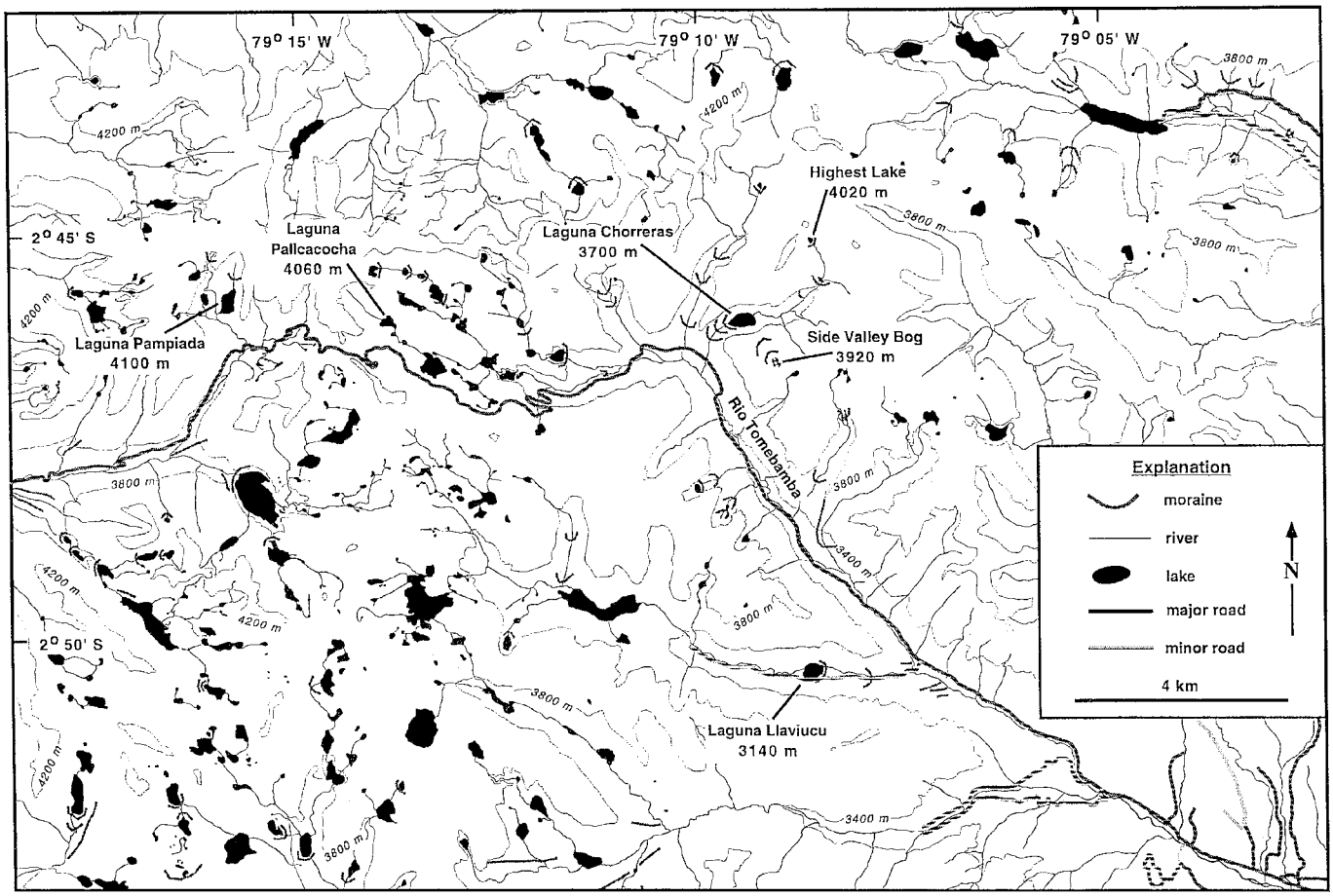

FIG. 2. Map of the region that includes Las Cajas National Park.

oxide paste to rid the surface of scratches that could affect analytical totals (Nebolini, 1996; Bagnato, 2000).

Electron microprobe analysis was used to determine the geochemical signature of all tephra layers. Although more time-consuming than bulk chemical assay, the electron microprobe enables grain-discrete measurements, and this avoids contamination from detrital grains in the tephras. Furthermore, because grain surfaces are polished before microprobe analysis, contamination from the alteration of shard surfaces during transport and deposition is eliminated (Hunt and Hill, 1993). Up to 45 grains of glass or of phenocrysts were analyzed for each tephra layer in each core. All analyses were made on a JEOL 733 Superprobe in the Earth and Environmental Sciences Department at Rensselaer Polytechnic Institute, Troy, New York. We used an accelerating voltage of 15 kV, a current of 5 ηamps, and a beam diameter of 5 μm. Wavelength dispersive spectrometry (WDS) was used to sequentially analyze nine major elements using five spectrometers. Counting time ranged from 10 to 40 s; calibration was performed on internal laboratory standards (Bagnato, 2000). Periodically, throughout an analysis session, an internal laboratory standard of rhyolitic glass from Yellowstone Park (USNM 72854) was analyzed to determine whether significant instrument drift had occurred; if so, recalibration was performed.

Sodium's volatilization during electron microprobe analysis of glass is widely recognized in tephra studies (e.g., Nielsen and Sigurdsson, 1981; Hunt and Hill, 1993; Delano *et al*., 1994, and references therein). Volatilization of Na is a function of the intensity, diameter, and duration of the incident electron beam (Hunt and Hill, 1993). For this reason, extra steps were taken to minimize and correct for sodium loss and the consequent overrepresentation of all other elements. The aforementioned electron microprobe settings were chosen in part to minimize sodium mobility, and these settings were used for all analyses. In addition, sodium was analyzed first and was analyzed 3–4 times at 10-s intervals during the course of each analysis. With these data, we empirically corrected all elemental concentrations for each analysis by fitting an exponential curve of sodium loss to beam exposure time and extrapolating Na concentration at $t = 0$ following Nielsen and Sigurdsson (1981). Finally, due to a number of possible causes, including the loss of other volatiles and poor beam focus, oxide totals rarely sum to 100 wt.%. To compare geochemical data from tephras made with different electron microprobes and under different

instrument conditions, it is important to normalize all results to a 100 wt.% total (Froggatt, 1992). However, as noted by Hunt and Hill (1993), normalization of poor data may lead to incorrect correlation of tephras. To avoid this problem, we excluded all results with analytical totals less than 90 wt.%. We chose this threshold because many tephras consistently reveal totals as low as ~90 wt.% that could not be attributed to operator error.

We used the similarity coefficient (SC) of Borchardt *et al.* (1972) as an objective and quantitative basis for correlating tephras among the lake and bog cores. This dimensionless index incorporates both the mean and the standard deviation of all elemental data and weighs elements according to the magnitude by which mean measured values exceed the detection limits of the electron microprobe and inversely by the relative deviation of mean values (Borchardt *et al.*, 1972; Bagnato, 2000). The SC of any given pair of geochemical analyses is expressed as a number from 0 to 1.0, where 1.0 is an identical match in both the mean *and* standard deviation of each of the nine elements analyzed. The closer the similarity coefficient is to 1.0, the greater the likelihood that a pair of tephras are indeed from the same unit. The SC is calculated as

$$d(A, B) = \frac{\sum_{i=1}^{i=n} Ri * gi}{\sum_{i=1}^{i=n} gi},$$

where: $d(A, B)$ = the similarity coefficient for samples A and B; i = element number; n = number of elements; $Ri = X_{iA}/X_{iB}$ if $X_{iB} > X_{iA}$, $Ri = X_{iB}/X_{iA}$ if $X_{iA} > X_{iB}$; X_{iA} = concentration of element i in sample A; X_{iB} = concentration of element i in sample B. The gi term, which ranges between 0 and 1, is designed to weigh the elemental data so that elements with well-defined mean values that greatly exceed probe detection limits contribute relatively more to the resultant SC. Thus, $gi = 1 - (((\sigma_{iA}/X_{iA})^2 + (\sigma_{iB}/X_{iB})^2)/E)^{1/2}$, where σ_{iA} and σ_{iB} are the standard deviations of element i in samples A and B. Finally, E is the relative error due to detection limit; $E = 1-$ (detection limit / (avg. X_{iA}, X_{iB})) (Bagnato, 2000).

Reliance on the SC as a basis for correlation requires estimation of maximum attainable SC values for each tephra. Because an SC value of 1.0 would require identical mean *and* standard deviation values for each of nine elements in a pair of tephras, and because of some inherent heterogeneity in the composition of any glass or phenocryst, it is virtually impossible to achieve an SC value of 1.0. To determine maximum attainable SC values for each tephra, we randomly divided the probe data from each of the six tephras present in the core from the Chorreras Valley Highest Lake (Fig. 2) into three subpopulations. SC values were then calculated among the three subpopulations for each tephra. Given that the subpopulations are from the same tephra, SC values would ideally be 1.0 for all three possible comparisons for each tephra. The extent to which calculated SC values are less than 1.0 is a reflection of some combination of the inherent chemical heterogeneity of the glass and the accuracy and precision of the electron microprobe. SC values for a given tephra unit in different lakes are unlikely to significantly exceed these maximum attainable SC values.

The age of each tephra was estimated from AMS ^{14}C dates from terrestrial macrofossils preserved in the cores. Because Laguna Pallcacocha is well dated (Rodbell *et al.*, 1999), most tephra age assignments are based on correlation to this core. In addition, basal dates were also obtained from each core and all well-preserved terrestrial macrofossils found in the other cores were also dated (Bagnato, 2000); these dates were also used in developing the tephrochronology.

RESULTS AND DISCUSSION

A variable number of tephras were found in the six cores studied. Seven tephras were found in the cores from Lagunas Pallcacocha, Chorreras, and Chorreras Valley Highest Lake (Figs. 2 and 3). Six tephras were found in the core from Laguna Pampiada, five were noted in the Laguna Llaviucu core, and only one tephra was observed in the Side Bog core. The paucity of tephras in the bog core may reflect wind or water erosion of tephra from the bog surface; in fact, the single tephra noted in this core was found in the lacustrine sediments at the base of the core (Fig. 3). The varying number of tephras in the lake cores may reflect variable core recovery. Because these cores comprise numerous nonoverlapping drives, up to ~10 cm of section that may include tephras may be missing between sequential drives. It is also possible that erosion of the lake floor by, for example, density driven undercurrents has removed one or more tephras from each coring locality.

Of the 33 tephras noted from all cores, 23 contain phenocrysts of either feldspar (18 tephras) or hornblende (eight tephras), or both (four tephras). Of the 23 phenocryst-containing tephras, six contain no glass. The glass compositions range as follows: ~67–78 wt.% in SiO_2, ~12–16 wt.% in Al_2O_3, and ~4–6 wt.% in Na_2O (Table 1). For any given tephra, feldspar phenocrysts possess much greater compositional variation than associated hornblende grains or glass. Owing to the general paucity of hornblende, we base our tephrochronology primarily on glass composition.

Sodium loss from glass shards with exposure to the microprobe beam varied within and among individual tephras (Fig. 4). Extrapolation of Na concentration to a beam time of 0 s resulted in Na estimates that are $\sim 10 \pm 7$ wt.% (mean $\pm 1\sigma$ of all samples) higher than uncorrected Na values (Table 1). This is substantially less than noted in other studies (e.g., Nielsen and Sigurdsson, 1981), which may be attributable to the relatively low probe current (5 nA) used in this study. The high degree of variability in the rate of Na loss with beam exposure indicates that Na volatility cannot be used as a diagnostic criterion for distinguishing tephras. Part of the variability in Na loss may be due to probe operator inconsistencies such as variations in the beam time needed to focus on individual glass shards. Even slight variations in the time that a grain is under the microprobe beam prior to analysis can have a significant impact on the

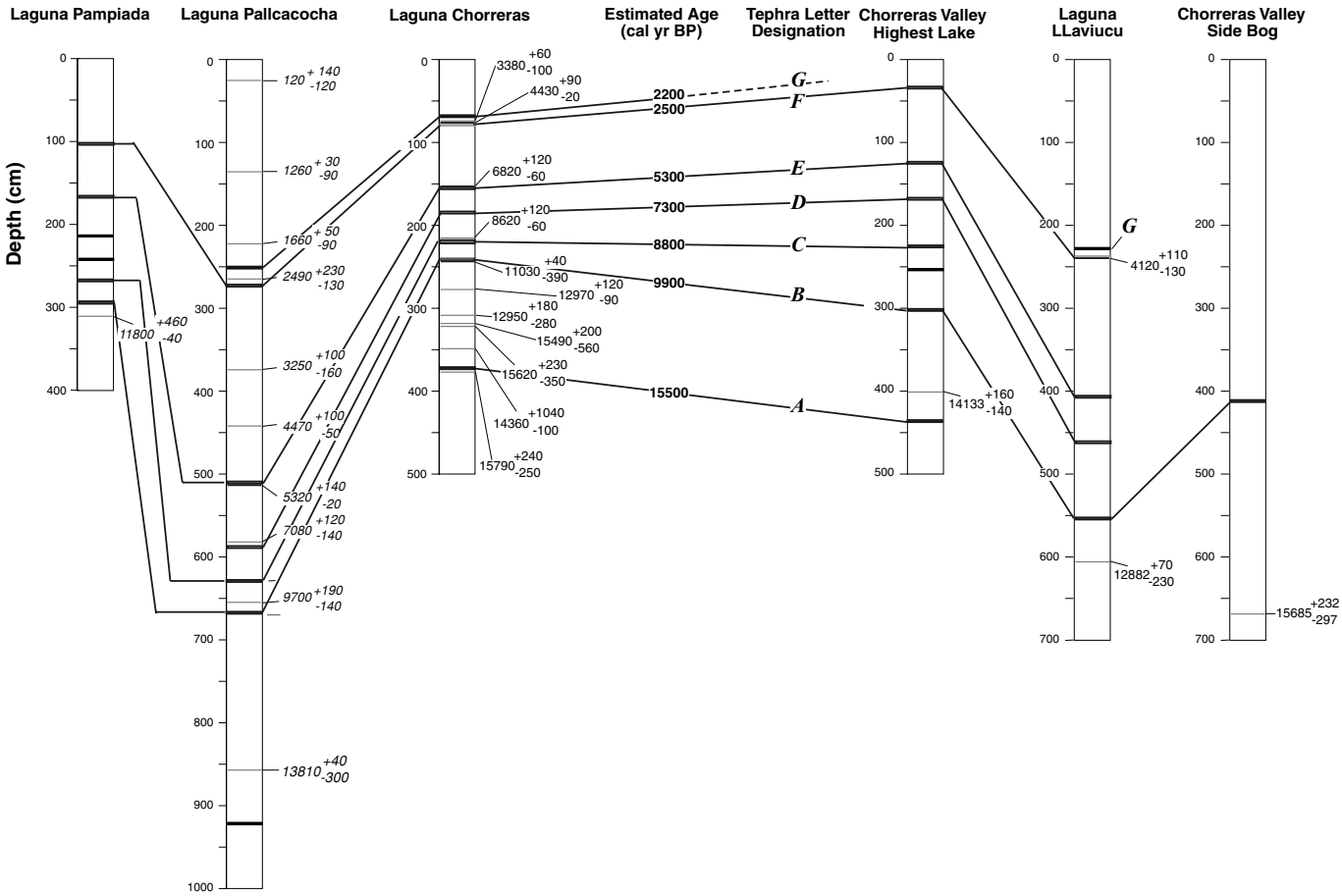

FIG. 3. Correlation of tephra in five lakes and one bog based on chemical composition. Radiocarbon ages in calibrated years B.P. are shown to the right of each section. Tephra that are correlated among two or more lakes are lettered A–G.

calculated Na loss because of the exponential nature of Na loss as noted by Nielsen and Sigurdsson (1981) and corroborated here (Fig. 4).

Maximum attainable SC values for glass as determined from pairs of randomly selected subpopulations of individual tephras from the Chorreras Valley Highest Lake core average 0.95 ± 0.02 ($\pm 1\sigma$). SC values for correlative tephras from the five lakes and one bog should be 0.95 ± 0.02. However, owing to the relatively small number of glass shards analyzed for each tephra in each core ($n \leq 45$; Table 1) coupled with the inherent geochemical variability of the glass component of all tephras, correlative tephras may fall outside the range of SC values noted here. Of the 49 tephras correlations made in this study, six yield SC values that fall slightly (0.01–0.03) below the predicted range of 0.95 ± 0.02 and one falls slightly (0.01) above this range; all others are 0.95 ± 0.02. A similar range of SC values were noted for correlative rhyolitic tephras preserved in lake sediment cores from southern British Columbia (Hallett *et al*., 2001).

SC values for all pairs of tephras from the five lakes and one bog reveal several prominent tephras and numerous other less widely preserved tephras (Fig. 3). Of the widespread tephras, tephra B (Fig. 3) is found in all six cores, tephras E and F are found in all of the lake cores but not in the bog core, tephras C and D are present in four of the five lake cores, and tephra G is found in three of the lake cores. Finally, tephra A is found in only two lakes, and four other tephras are found only in a single core. Correlation of tephras among the cores is straightforward; commonly, only one high SC value (>0.90) is found among all possible matches (bold entries, Table 2). In cases where multiple possible correlations exist, stratigraphic position generally precludes all but one of the possible matches. Tephra F, which is present in all of the lake cores, is the most conspicuous because it is the thickest (~1.0 to 1.3-cm thick) and contains hornblende phenocrysts. SC values for the glasses range from 0.94 to 0.96; SC values for the hornblende phenocrysts range from 0.91 to 0.96. Hornblende phenocrysts have only been noted in this tephra and in much older tephras in cores from Laguna Pampiada, Highest Lake, and Side Bog (Table 1). Two other of the widespread tephras have a distinct composition; tephra B is the most silica-rich (76.5–78.0 wt.%) whereas tephra E is the least silica rich (67–69 wt.%).

TABLE 1
Major Element Geochemistry of Glass and Phenocrysts in Tephras from Lakes in Las Cajas National Park

Lake (Fig. 2)	Depth (cm)	Material and no. of analyses	Weight Percentage (mean/1σ) SiO_2	TiO_2	Al_2O_3	FeO	MnO	MgO	CaO	Na_2O	K_2O	Total[a]	Na correction[b] (%; mean/1σ)
Chorreras	67.5	Feldspar	53.54	0.17	28.47	0.74	0.07	0.20	11.53	4.97	0.32	100.0	
		$n = 24$	1.28	0.15	0.87	0.12	0.04	0.04	0.90	0.46	0.09		
		Feldspar	59.16	0.85	19.82	4.57	0.12	1.66	6.70	5.54	1.69	100.1	
		$n = 9$	0.40	0.47	4.53	2.89	0.05	1.12	1.17	1.06	0.73		
		Feldspar	58.25	0.30	25.46	0.98	0.08	0.30	8.33	6.56	0.76	101.0	
		$n = 5$	2.01	0.17	1.08	0.96	0.04	0.31	0.70	1.01	0.16		
	78.0	Glass	72.88	0.25	15.32	1.83	0.11	0.63	2.72	4.73	1.56	98.8	7.67
		$n = 19$	0.95	0.07	0.30	0.21	0.03	0.14	0.27	0.61	0.10		3.54
		Hornblende	45.05	1.43	12.20	15.38	0.15	13.13	10.30	2.07	0.29	97.1	
		$n = 21$	0.72	0.24	0.64	1.00	0.18	0.72	0.33	0.17	0.05		
		Feldspar	58.43	0.08	26.05	0.31	0.05	0.04	8.12	6.06	0.27	99.4	
		$n = 23$	2.77	0.06	3.64	0.29	0.03	0.09	2.07	0.98	0.29		
	155.0	Glass	67.86	0.73	15.47	3.76	0.13	1.05	3.39	4.54	2.60	99.5	6.91
		$n = 20$	1.11	0.14	1.17	0.51	0.04	0.26	0.66	0.37	0.22		3.24
	185.0	Glass	75.02	0.17	14.40	1.04	0.13	0.27	1.33	4.75	2.91	100.5	8.11
		$n = 16$	0.66	0.07	0.42	0.13	0.02	0.06	0.12	0.59	0.13		2.43
		Feldspar	54.66	0.07	29.04	0.57	0.03	0.09	11.95	5.00	0.22	101.6	
		$n = 5$	1.23	0.08	0.76	0.17	0.04	0.04	0.89	0.30	0.05		
	218.0	Glass	76.16	0.23	13.65	0.95	0.13	0.27	1.02	4.59	3.02	96.3	7.66
		$n = 36$	0.54	0.11	0.18	0.08	0.05	0.02	0.08	0.57	0.11		4.04
		Feldspar	54.51	0.29	29.46	0.60	0.08	0.18	12.09	5.10	0.21	102.5	
		$n = 4$	0.96	0.14	0.23	0.12	0.03	0.05	0.91	0.38	0.05		
		Feldspar	61.71	0.12	25.25	0.21	0.07	0.11	6.42	8.16	0.38	102.4	
		$n = 4$	0.43	0.16	0.18	0.04	0.04	0.02	0.32	0.64	0.05		
	242.0	Glass	78.08	0.24	12.24	0.87	0.07	0.16	0.81	3.46	4.07	95.4	4.28
		$n = 38$	0.87	0.09	0.79	0.08	0.03	0.02	0.06	0.29	0.13		2.68
		Feldspar	55.66	0.03	27.61	0.50	0.04	0.04	9.64	5.47	0.33	99.3	
		$n = 2$	2.91	0.00	1.75	0.11	0.01	0.02	2.28	1.34	0.13		
	373.0	Glass	77.20	0.17	12.78	0.76	0.07	0.14	0.97	4.25	3.69	93.7	6.51
		$n = 7$	0.21	0.07	0.11	0.06	0.02	0.01	0.06	0.19	0.09		2.97
Pallcacocha	251.8	Feldspar	53.89	0.10	28.76	0.69	0.05	0.09	11.64	4.89	0.28	100.40	
		$n = 26$	1.08	0.07	0.69	0.10	0.03	0.03	0.66	0.49	0.05		
	269.0	Glass	72.52	0.35	15.67	1.73	0.11	0.59	2.59	4.92	1.54	99.3	5.75
		$n = 25$	1.15	0.14	1.37	0.16	0.04	0.07	0.15	0.56	0.10		2.03
		Hornblende	43.45	1.22	11.75	15.22	0.26	12.59	10.18	2.15	0.26	97.1	
		$n = 11$	0.61	0.21	0.60	0.55	0.05	0.37	0.17	0.13	0.03		
		Feldspar	55.01	0.15	28.67	0.64	0.08	0.19	11.13	5.61	0.29	101.8	
		$n = 6$	2.30	0.10	1.32	0.11	0.02	0.01	1.21	0.71	0.07		
	507.3	Glass	67.62	0.84	15.36	3.62	0.13	1.10	3.05	5.58	2.73	98.2	9.74
		$n = 13$	1.25	0.23	0.62	0.38	0.03	0.13	0.39	0.49	0.22		4.43
		Feldspar	55.01	0.15	28.67	0.64	0.08	0.19	11.13	5.61	0.29	101.8	
		$n = 6$	2.30	0.10	1.32	0.11	0.02	0.01	1.21	0.71	0.07		
	588.8	Glass	74.53	0.18	13.98	1.03	0.15	0.41	1.27	5.58	2.93	99.4	24.35
		$n = 24$	1.61	0.07	1.16	0.26	0.05	0.25	0.37	0.57	0.37		3.47
		Feldspar	60.08	0.10	26.01	0.27	0.07	0.12	7.61	7.14	0.32	101.7	
		$n = 8$	0.89	0.05	0.37	0.07	0.02	0.01	0.47	0.36	0.05		
	630.7	Glass	75.72	0.16	13.41	0.93	0.14	0.27	1.01	5.38	3.05	94.7	29.09
		$n = 19$	0.28	0.07	0.11	0.07	0.05	0.02	0.07	0.30	0.11		3.79
		Feldspar	56.53	0.11	26.83	0.46	0.12	0.15	9.34	5.96	0.31	99.8	
		$n = 4$	5.61	0.11	3.13	0.32	0.02	0.06	4.26	2.31	0.15		
	667.5	Glass	77.73	0.24	12.05	0.89	0.07	0.20	0.79	3.94	4.09	95.5	13.18
		$n = 24$	0.36	0.09	0.21	0.09	0.03	0.06	0.06	0.36	0.12		8.45
		Feldspar	57.81	0.07	26.41	0.39	0.07	0.13	8.68	6.11	0.43	100.1	
		$n = 12$	2.19	0.04	1.28	0.06	0.04	0.03	1.56	0.80	0.11		
	921.0	Feldspar	54.84	0.13	27.26	0.75	0.07	0.18	10.21	5.15	0.50	99.1	
		$n = 15$	1.97	0.06	1.35	0.22	0.04	0.06	1.62	0.85	0.15		
Llaviucu	227.0	Feldspar	60.01	1.31	16.00	6.60	0.17	2.53	5.21	4.73	2.49	99.0	
		$n = 15$	1.44	0.15	0.76	0.78	0.03	0.66	0.61	0.39	0.25		
	238.0	Glass	72.80	0.25	15.19	1.64	0.09	0.53	2.63	5.26	1.64	98.1	11.39
		$n = 27$	0.66	0.15	0.51	0.12	0.04	0.04	0.10	0.55	0.20		6.07

TABLE 1—*Continued*

Lake (Fig. 2)	Depth (cm)	Material and no. of analyses	Weight Percentage (mean/1σ) SiO_2	TiO_2	Al_2O_3	FeO	MnO	MgO	CaO	Na_2O	K_2O	Total[a]	Na correction[b] (%; mean/1σ)
		Hornblende	43.03	1.14	12.53	14.49	0.25	12.58	10.75	2.07	0.28	97.1	
		$n = 13$	0.99	0.29	1.11	1.52	0.06	1.03	0.65	0.20	0.03		
		Feldspar	56.23	0.01	27.34	0.20	0.02	0.01	9.50	6.34	0.14	99.8	
		$n = 14$	1.18	0.03	0.67	0.06	0.02	0.01	0.87	0.51	0.03		
	406.0	Glass	69.11	0.69	14.83	3.19	0.12	0.91	2.92	5.51	2.76	98.4	13.85
		$n = 22$	1.86	0.19	0.53	0.58	0.04	0.19	0.51	0.63	0.16		7.40
		Feldspar	55.13	0.10	27.99	0.57	0.05	0.05	10.67	5.44	0.26	100.3	
		$n = 9$	1.30	0.11	0.77	0.07	0.03	0.01	0.96	0.62	0.05		
	461.0	Glass	74.81	0.21	14.03	0.95	0.11	0.26	1.30	5.50	2.87	98.6	15.53
		$n = 22$	1.23	0.11	0.79	0.13	0.03	0.05	0.37	0.50	0.26		3.25
	553.0	Glass	78.01	0.25	11.95	0.82	0.06	0.15	0.82	3.95	4.01	96.0	8.67
		$n = 34$	0.60	0.13	0.24	0.09	0.03	0.01	0.09	0.52	0.15		6.82
Pampiada	102.5	Glass	72.05	0.23	15.22	2.04	0.06	0.90	2.90	5.01	1.59	94.6	6.37
		$n = 16$	2.75	0.13	0.64	1.26	0.03	1.25	0.75	0.36	0.15		5.14
		Hornblende	44.23	1.31	12.03	14.73	0.30	11.83	10.20	2.01	0.37	97.0	
		$n = 33$	2.60	0.24	0.55	1.51	0.07	1.17	0.62	0.23	0.10		
	166.5	Glass	67.05	0.79	16.08	3.59	0.09	1.12	3.47	5.27	2.56	96.3	4.39
		$n = 37$	3.01	0.21	2.80	0.86	0.04	0.36	1.47	0.70	0.49		4.48
	215.0	Glass	73.26	0.28	15.08	1.65	0.08	0.55	2.59	4.85	1.68	96.9	4.34
		$n = 24$	2.73	0.15	1.26	0.48	0.04	0.18	0.31	0.36	0.56		1.85
		Hornblende	44.92	1.23	12.87	14.40	0.30	11.43	10.09	2.35	0.30	97.9	
		$n = 14$	3.91	0.34	3.47	4.06	0.10	3.30	0.82	1.34	0.03		
	241.0	Feldspar	55.63	0.27	17.34	4.32	0.15	6.67	10.94	4.23	0.43	96.3	
		$n = 17$	4.79	0.28	12.07	5.68	0.18	9.48	6.22	3.21	0.43		
	268.5	Glass	76.47	0.15	13.59	0.84	0.08	0.19	1.05	4.61	3.04	95.3	4.98
		$n = 38$	0.33	0.08	0.17	0.08	0.03	0.16	0.07	0.26	0.15		2.48
	294.0	Glass	77.58	0.25	12.46	0.81	0.04	0.17	1.05	3.55	4.09	94.6	4.42
		$n = 30$	2.68	0.08	1.76	0.07	0.03	0.12	1.15	0.50	0.45		2.07
Chorreras Valley Highest Lake	33.0	Glass	71.41	0.51	15.62	1.86	0.06	0.77	3.04	5.25	1.49	95.0	3.26
		$n = 45$	2.93	0.17	3.73	1.63	0.03	0.79	1.25	2.37	0.27		2.56
		Hornblende	43.42	1.19	11.79	15.27	0.31	12.42	9.72	2.80	0.32	97.2	
		$n = 20$	1.03	0.26	1.04	0.84	0.08	0.72	0.27	0.17	0.05		
	124.5	Glass	67.79	0.72	15.53	3.66	0.11	1.08	3.58	4.95	2.60	96.3	3.73
		$n = 28$	2.75	0.19	2.37	0.69	0.04	0.26	1.47	0.22	0.47		1.19
	169.5	Glass	74.17	0.26	14.51	1.00	0.08	0.25	1.62	5.38	2.75	97.9	12.97
		$n = 34$	2.37	0.07	1.51	0.24	0.03	0.09	0.81	0.77	0.52		5.99
	226.0	Glass	76.43	0.36	13.49	0.74	0.07	0.17	1.12	4.72	2.92	95.1	7.06
		$n = 22$	1.49	0.15	0.95	0.15	0.03	0.03	0.28	0.68	0.27		2.47
		Hornblende	47.04	2.13	9.70	8.43	0.25	12.10	17.29	1.70	0.71	99.4	
		$n = 33$	6.01	1.28	5.23	2.40	0.09	3.60	6.03	1.43	0.83		
	253.0	Feldspar	54.66	0.17	26.43	0.49	0.02	0.12	9.31	5.48	0.89	97.6	
		$n = 24$	9.55	0.17	5.97	0.19	0.02	0.04	3.50	1.45	1.32		
	303.5	Glass	77.21	0.24	12.47	0.77	0.03	0.20	0.94	4.16	3.99	94.8	2.32
		$n = 35$	1.38	0.11	0.99	0.11	0.02	0.09	0.49	0.48	0.28		2.75
		Feldspar	52.73	0.92	15.78	6.39	0.17	7.53	8.96	4.48	0.82	97.8	
		$n = 20$	6.65	0.78	9.13	5.86	0.16	7.52	2.42	2.30	0.89		
	436.0	Glass	75.99	0.22	13.20	0.75	0.05	0.14	1.14	4.94	3.61	95.5	20.09
		$n = 27$	1.42	0.06	0.90	0.12	0.02	0.03	0.41	0.45	0.29		5.42
Chorreras Valley Side Bog	411.0	Glass	77.18	0.33	12.20	0.85	0.04	0.20	0.98	4.19	4.05	95.0	22.45
		$n = 35$	1.32	0.10	0.98	0.24	0.03	0.35	0.43	0.38	0.25		5.60
		Hornblende	46.92	1.78	8.79	11.51	0.29	13.85	11.03	1.82	0.49	96.48	
		$n = 40$	2.96	0.54	4.51	2.71	0.08	3.35	0.51	1.06	0.10		

[a] The totals indicated are all for unnormalized data; the phenocryst data are unnormalized whereas the glass data have been corrected for Na loss and normalized to a 100% total; these data were used to calculate similarity coefficient values (Table 2).

[b] Na correction is the average difference between the extrapolated Na content at $t = 0$ and the measured Na content at ~10-s beam exposure as a percentage of the measured (10-s) Na value. The values given are the average amount (and $\pm 1\sigma$) by which Na has been increased for a glass of a given tephra.

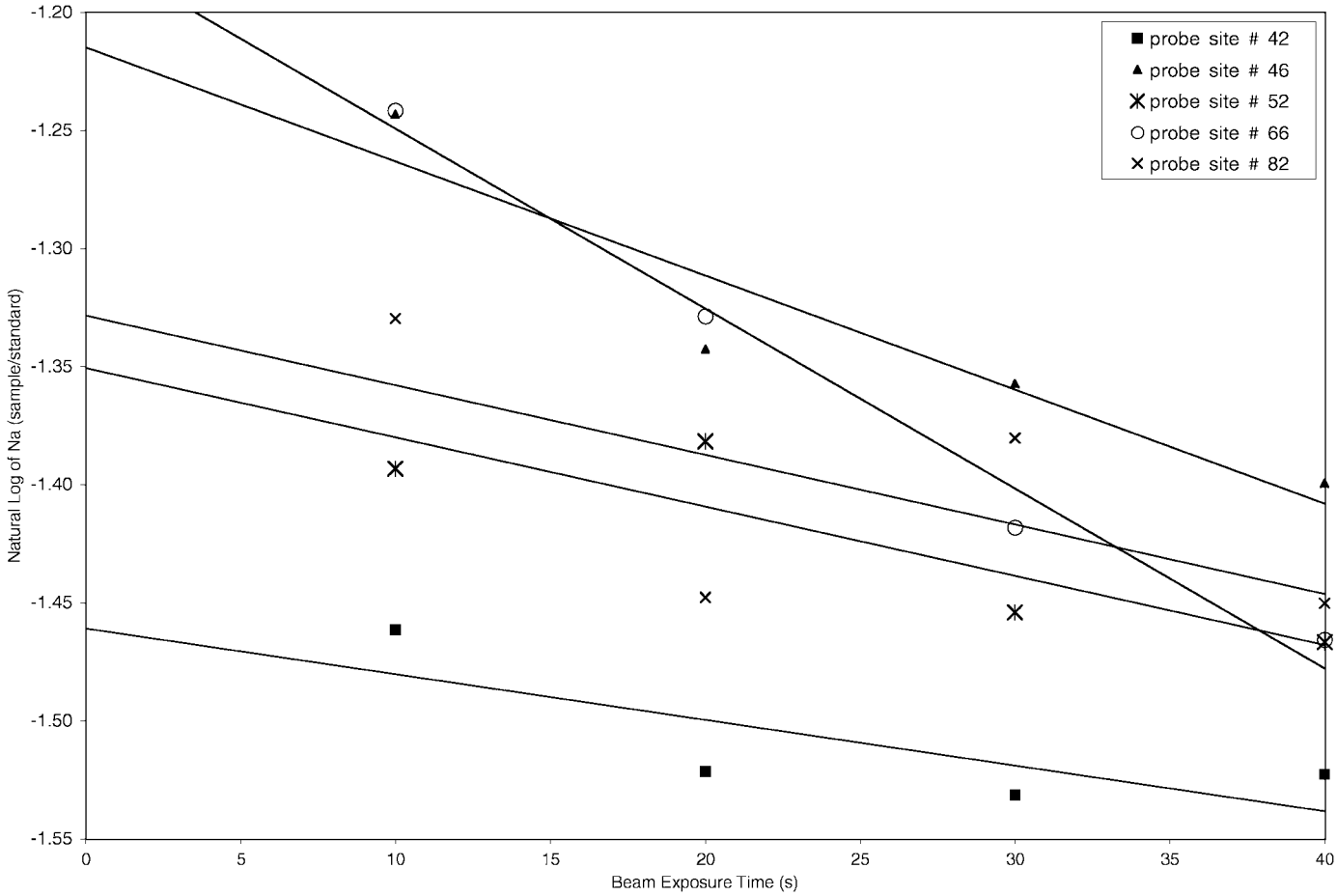

FIG. 4. Decay of sodium in glass with exposure to electron microprobe beam at 15 kV and 5n A for five probe sites on glass shards from tephra F in Chorreras Valley Highest Lake (Fig. 3). Extrapolation to origin provides an empirical means of correcting for Na loss following Nielsen and Sigurdsson (1981).

Twenty-six radiocarbon dates from plant macrofossils preserved in the six cores (Table 3) provide the basis for a preliminary regional tephrochronology and highlight some of the complications that arise from reliance on terrestrial plant macrofossils for dating lacustrine sediment cores. Radiocarbon dates generally yield stratigraphically consistent limiting age estimates for correlative tephras. In two cases, however, limiting radiocarbon dates from Laguna Chorreras are not consistent and may reflect reworking of old carbon from the many peatlands located upvalley from this lake. Tephra E is the older of these two problematic tephras; as noted above, this tephra is easily distinguished from all others by its relatively low SiO_2 content (67–69 wt.%), and SC values among all lake cores range from 0.91–0.98. In the Laguna Pallcacocha core, tephra E is immediately above an interval radiocarbon dated to 5320 (+140; −20) cal yr B.P., yet in the Laguna Chorreras core this tephra is found immediately below an interval dated to 6820 (+120; −60) cal yr B.P. (Fig. 3). Similarly, the radiocarbon dates on tephra F also appear anomalously old in the Laguna Chorreras core. In the Pallcacocha core tephra F, which is clearly identified in all lakes by being the thickest and by the presence of horneblende phenocrysts, is found between two intervals that yield radiocarbon dates of 3250 (+100; −160) cal yr B.P. and 2490 (+230; −130) cal yr B.P. (Fig. 3). In contrast, tephra F in the Laguna Chorreras core (SC = 0.97) is found immediately below an interval that yields a radiocarbon age of 4430 (+90; −20) cal yr B.P. (Fig. 3). Tephra F in the Llaviucu core, which yields SC values of 0.94 and 0.95 when compared with the Chorreras and Pallcacocha cores, respectively, is found immediately above an interval dated to 4120 (+110; −130) cal yr B.P.

In the absence of any source of old carbon that could generate a significant hardwater effect in Laguna Chorreras, we suggest that one likely source of old carbon is from the recycling of organic matter from the numerous peatlands that are located upvalley from Laguna Chorreras. Most of these peat deposits are at least 1.5 m thick, and lateral channel migration by the main stream that drains the Chorreras Valley undoubtedly has periodically eroded these deposits and transported aged organic matter into the Lake. A ∼10-cm-thick section in the late glacial portion of the Laguna Chorreras core appears to provide a good example of such an event. Upcore from a depth of ∼325 cm,the sediment

TABLE 2
Similarity Coefficients for Glass from All Tephras

Core Depth (cm)	78.0	155.0	185.0	218.0	242.0	373.0	269.0	507.3	588.8	630.7	667.5	238.0	406.0	461.0	553.0	102.5	166.5	215.0	268.5	294.0	33.0	124.5	169.5	226.0	303.5	436.0	411.0
			Laguna Chorreras																								
78.0	1.00																										
155.0	0.75	1.00																									
185.0	0.73	0.69	1.00																								
218.0	0.68	0.65	0.93	1.00																							
242.0	0.57	0.53	0.76	0.81	1.00			Laguna Pallcacocha																			
373.0	0.60	0.58	0.80	0.85	0.89	1.00																					
269.0	**0.97**	0.75	0.72	0.67	0.56	0.59	1.00																				
507.3	0.74	**0.94**	0.68	0.63	0.52	0.56	0.74	1.00				Laguna Llaviucu															
588.8	0.73	0.71	**0.94**	0.90	0.76	0.80	0.74	0.73	1.00																		
630.7	0.66	0.64	0.92	**0.97**	0.80	0.84	0.66	0.65	0.92	1.00																	
667.5	0.60	0.56	0.80	0.85	**0.95**	0.88	0.59	0.55	0.78	0.84	1.00																
238.0	**0.94**	0.75	0.73	0.68	0.57	0.60	**0.95**	0.76	0.77	0.69	0.60	1.00					Laguna Pampiada										
406.0	0.78	**0.91**	0.72	0.67	0.55	0.60	0.77	**0.93**	0.77	0.69	0.58	0.79	1.00														Chorreras
461.0	0.70	0.68	**0.95**	0.93	0.77	0.80	0.70	0.70	**0.95**	0.94	0.80	0.73	0.73	1.00								Chorreras Highest Lake					Side
553.0	0.58	0.55	0.77	0.82	**0.96**	0.92	0.57	0.53	0.77	0.81	**0.95**	0.58	0.57	0.77	1.00												Bog
102.5	**0.97**	0.85	0.77	0.72	0.62	0.67	**0.96**	0.85	0.76	0.72	0.64	**0.95**	0.86	0.76	0.64	1.00											
166.5	0.73	**0.96**	0.67	0.63	0.53	0.57	0.74	**0.96**	0.71	0.65	0.56	0.76	**0.91**	0.68	0.55	0.84	1.00										
215.0	0.95	0.78	0.76	0.71	0.60	0.64	0.97	0.77	0.77	0.70	0.62	0.97	0.80	0.74	0.61	0.95	0.76	1.00									
268.5	0.70	0.69	0.91	**0.97**	0.85	0.92	0.69	0.68	0.90	**0.95**	0.86	0.70	0.71	**0.91**	0.87	0.72	0.69	0.73	1.00								
294.0	0.65	0.61	0.81	0.85	**0.97**	0.92	0.64	0.60	0.80	0.83	**0.95**	0.65	0.63	0.81	**0.96**	0.69	0.60	0.69	0.88	1.00							
33.0	**0.95**	0.84	0.75	0.72	0.62	0.67	**0.95**	0.84	0.76	0.73	0.63	**0.95**	0.85	0.77	0.63	**0.96**	0.84	0.93	0.71	0.69	1.00						
124.5	0.75	**0.98**	0.69	0.65	0.54	0.58	0.75	**0.94**	0.71	0.65	0.55	0.75	**0.91**	0.68	0.56	0.85	**0.96**	0.78	0.70	0.61	0.84	1.00					
169.5	0.74	0.69	**0.94**	0.90	0.75	0.78	0.75	0.71	**0.94**	0.92	0.78	0.78	0.75	**0.96**	0.76	0.81	0.70	0.78	0.88	0.80	0.81	0.70	1.00				
226.0	0.66	0.64	0.88	**0.90**	0.84	0.90	0.65	0.62	0.88	0.88	0.83	0.66	0.66	0.88	0.86	0.74	0.63	0.69	**0.96**	0.86	0.73	0.65	0.86	1.00			
303.5	0.63	0.61	0.82	0.87	**0.92**	0.95	0.63	0.59	0.81	0.86	**0.95**	0.64	0.63	0.82	**0.94**	0.68	0.60	0.67	0.90	**0.96**	0.68	0.61	0.80	0.89	1.00		
436.0	0.63	0.61	0.84	0.86	0.86	**0.95**	0.64	0.59	0.85	0.86	0.85	0.65	0.63	0.84	0.89	0.73	0.60	0.68	0.93	0.89	0.72	0.62	0.83	0.93	0.90	1.00	
411.0	0.67	0.64	0.84	0.90	**0.94**	**0.96**	0.67	0.63	0.82	0.88	**0.96**	0.67	0.66	0.83	**0.96**	0.68	0.63	0.70	0.91	**0.96**	0.67	0.65	0.81	0.88	**0.97**	0.91	1.00

Note. Bold values indicate correlation used in Figures 3 and 5.

TABLE 3
AMS Radiocarbon Dates from Plant Macrofossils in Sediment Cores

Lake/Bog	Depth below mud surface (cm)	Radiocarbon age (^{14}C yr B.P.)	±(^{14}C yr B.P.)	Radiocarbon age (cal yr B.P.)[a]	Age uncertainty (-1σ; cal yr)	Age uncertainty ($+1\sigma$; cal yr)	Lab no.	Reference
Chorreras	74–75	3180	50	3380	100	70	CAMS-26405	this study
	77.5	4010	60	4430	20	90	CAMS-10028	this study
	154–156	6050	60	6820	60	120	CAMS-26406	this study
	215–217	7880	60	8620	60	120	CAMS-26407	this study
	243–245	9540	60	11030	390	40	CAMS-26415	this study
	278–279	10960	60	12970	90	120	CAMS-34964	this study
	309–311	10930	160	12950	280	180	CAMS-11956	this study
	319–320	12880	70	15490	560	200	CAMS-11957	this study
	322–323	13010	70	15620	350	230	CAMS-34963	this study
	348–350	12470	80	14360	100	1040	CAMS-11958	this study
	379–381	13160	80	15790	250	240	CAMS-34965	this study
Pallcacocha	25.5–26.5	100	60	120	120	140	CAMS-34966	Rodbell *et al*., 1999
	136–137	1320	60	1260	90	30	CAMS-34967	Rodbell *et al*., 1999
	223–224.5	1760	50	1660	90	50	CAMS-34968	Rodbell *et al*., 1999
	264–268	2480	60	2490	130	230	CAMS-26408	Rodbell *et al*., 1999
	374.5–375.5	3060	60	3250	160	100	CAMS-34969	Rodbell *et al*., 1999
	443–444	4040	55	4470	50	100	AA-24011	Rodbell *et al*., 1999
	508.5–509.5	4645	65	5320	20	140	AA-24012	Rodbell *et al*., 1999
	582.5–583	6185	65	7080	140	120	AA-24013	Rodbell *et al*., 1999
	656.5	8753	63	9700	140	190	AA-27026	Rodbell *et al*., 1999
	858.6	11770	70	13810	300	40	CAMS-11967	Rodbell *et al*., 1999
Laguna Llaviucu	237–240	3780	60	4120	130	110	CAMS-26404	this study
	600–606	10800	60	12880	230	70	CAMS-26414	this study
Laguna Pampiada	309–310	10210	60	11800	40	460	CAMS-26409	this study
Chorreras Highest Lake	401–402	12220	60	14130	40	1070	CAMS-26412	this study
Chorreras Valley Side Bog	668–670	13070	60	15680	300	230	CAMS-26411	this study

[a] We used Calib 4.0 of Stuiver *et al*. (1998) to calibrate radiocarbon dates to an approximately calendrical time scale.

changes abruptly from an organic-rich gyttja (10–15 wt.% organic carbon) to an inorganic silt containing abundant very small fragments of plant macrofossils. Two radiocarbon dates from this material yielded nearly identical ages of ~15,620 (+230; −350) and 15,490 (+200; −560) cal yr B.P., which are more than 1000 yr older than radiocarbon dates from the gyttja either above or below this interval.

Because of the apparent problem arising from the recycling of organic matter on the landscape, we have based much of our chronology on the laminated core from Laguna Pallcacocha (Rodbell *et al*., 1999). This lake is located in the floor of a cirque that is surrounded by steep slopes with little, if any, peat deposits. We have encountered no radiocarbon reversals such as those noted above or reported from the closely spaced dating of a core from Laguna Llaviucu by Colinvaux *et al*. (1997). Linear interpolation between dated intervals in the Pallcacocha core indicates that the most widespread tephras (B-G, Fig. 3) were deposited approximately 9900, 8800, 7350, 5300, 2500, and 2200 cal yr B.P. Based on linear extrapolation of sedimentation rates, tephra A was deposited ~15,500 cal yr B.P., and the noncorrelatable tephra near the base of the Pallcacocha core was deposited ~15,100 cal yr B.P. (Fig. 3).

Comparison of principal major element abundances in the tephras preserved in the six cores reveals a general trend toward decreasing SiO_2 content and increasing Al_2O_3 content through the Holocene (Fig. 5). This trend is best exemplified by tephras B–E (Fig. 5). Whether this reflects magmatic evolution from a single source or the serendipity of distinct sources with progressively lower silica content hinges on interpretations of the number of sources responsible for the tephras. Whereas a progressive decline in silica content during a single eruption has been widely documented and reflects chemical zonation of magma chambers (e.g., Francis, 1993), this trend has not been widely reported for eruptions from a single source but separated by thousands of years.

Correlation of the distal tephras documented in this study with proximal tephras and possible source vents in central and northern Ecuador is hindered by a general lack of geochemical data from the latter. Moreover, the zoned nature of proximal tephras, which may be many 10s of meters thick, makes it unlikely that a close geochemical match is attainable. In the absence of isopach maps of tephras throughout central and southern Ecuador, correlation among distal tephras in southern Ecuador with the numerous proximal tephras and source vents in the northern part

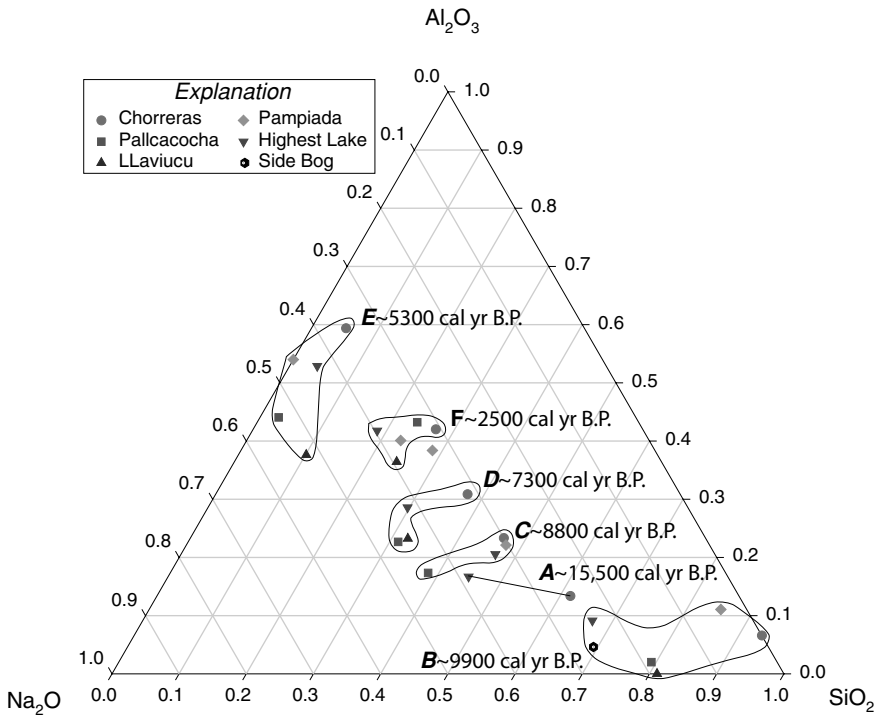

FIG. 5. Ternary diagram of SiO_2, Al_2O_3, and Na_2O for glass from correlative tephra in cores from five lakes and one bog in Las Cajas National Park. Data were rescaled to accentuate subtle differences in tephra composition. Mean values (MV) of each oxide for each tephra layer in each core were rescaled so that $MV^* = MV - MV_{min} \times (MV_{max} - MV_{min})^{-1}$, where MV^* is the rescaled mean value of an oxide, MV_{max} is the maximum mean value of that oxide in the entire suite of samples analyzed, and MV_{min} is the minimum mean value of that oxide. Finally, for ternary plotting purposes, the resultant MV^* values for SiO_2, Al_2O_3, and Na_2O were rescaled so that the sum of these oxides equals one. Letters denote correlation of tephras as in Figure 3.

of the country can only be tentatively made on chronologic grounds.

Although there are no comparable electron microprobe data from tephras on the flanks of the active volcanoes of central and northern Ecuador, several radiocarbon-dated tephras on the active volcanoes appear to correlate with distal tephras documented in this study. Tephra *F* on the flanks of Volcán Cotopaxi (Fig. 1), which contains rhyolitic glass and was deposited ~7000 cal yr B.P. (Hall and Mothes, 1994) may correlate with the similar-age rhyolitic glass (tephra D in Figs. 3 and 5) noted in four of the five lakes of this study. Likewise, the andesitic ashfalls *GF* on the flanks of Cotopaxi (Hall and Mothes, 1994), which date to ~5400 cal yr B.P., may correlate with the widespread low-silica tephras deposited in all of the lakes in this study at about the same time (tephra E in Figs. 3 and 5). Finally, Tephra *NIN-A* (Hall and Mothes, 1994) on the flanks of Volcán Ninahuilca (Fig. 1), which contains vesicular glass and hornblende, appears to correlate well with the prominent hornblende-containing tephras deposited ~2500 cal yr B.P. in all of the lakes of the present study (tephra F in Figs. 3 and 5).

The lack of tephras in the sediment cores of this study that are correlatable with any of the numerous proximal tephras deposited during the last two millennia (Hall and Mothes, 1994) suggests that the eruptions that produced the distal tephras noted in this study were either especially large or occurred when wind directions were favorable to transport tephras at least 150 km to the south. Prevailing wind directions generally are E–W across the axis of the Andes, but during the austral summer moisture-bearing air masses do travel southward along the eastern side of the Andes. In either case, the distal tephras noted in this study are the product of an unusual set of circumstances, which have not been repeated in the past ~2000 yr: unusually voluminous eruptions, strongly prevailing southward winds, or both.

CONCLUSIONS

Six widespread tephras (~0.1–1.0 cm thick) with rhyolitic to dacitic glass and/or phenocrysts of feldspar or hornblende are preserved in the glacial lakes of Las Cajas National Park, southern Ecuador. In addition to the tephras found in all or most of the sites, there are several tephras that can only be found in one or two of the lake basins studied. The widely recorded tephras were deposited 9900, 8800, 7300, 5300, 2500, and 2200 cal yr B.P. The oldest tephras were deposited ~15,500 and 15,100 cal yr B.P. and are not found in all cores. The composition of the glass from each tephra as determined by electron microprobe measurements is sufficiently unique to yield unambiguous correlation among all lake basins. Sodium loss with beam exposure, which, if uncorrected, would cause an ~10 wt.% underestimation of Na, must be accounted for when comparing

the composition of other tephras to those reported here. Similarity coefficients based on nine major elements from correlative glass samples are ∼0.95 (±0.02). Of the 26 AMS ^{14}C dates from plant macrofossils, those from Laguna Pallcacocha appear to provide the most reliable age control. Several dates from Laguna Chorreras appear to be anomalously old, which we attribute to the reworking of aged organic matter from upvalley peatlands. Correlation of the distal tephras documented here with the thick proximal volcaniclastic strata documented on the flanks of volcanoes in central and northern Ecuador is hindered by a general paucity of geochemical data on the latter; however, several tephras appear to correlate with major eruptions of Volcán Cotopaxi and Volcán Ninahuilca. The tephrochronology determined here provides a geochronologic starting point for late Quaternary stratigraphic studies in southern Ecuador.

ACKNOWLEDGMENTS

This research was funded by grants from the U.S. National Science Foundation to DTR (EAR-9418886 and ATM-9809229) and GOS (EAR-9422424 and ATM-9813969) and by funds from the Union College Internal Education Foundation (to SB and JCN). We thank D. Wark and K. Becker of the Electron Microprobe Laboratory of the Department of Earth and Environmental Sciences at Rensselaer Polytechnic Institute (Troy, NY) for instruction with operating the microprobe and to J. Garver (Union College) for guidance on polishing probe targets. Finally, M. Hall and P. Mothes of the Instituto Geofisico, Escuela Politecnica Nacional in Quito, Ecuador, provided advice in the early stages of our work in Ecuador. The manuscript benefited substantially from the careful reviews of Franklin F. Foit Jr. and W. E. Scott.

REFERENCES

Bagnato, S. (2000). "Tephrochronology of late Quaternary sediment cores from southern Ecuador." Unpublished B.S. thesis, Union College, Schenectady, NY.

Barazangi, M., and Isacks, B. L. (1976). Spatial distribution of earthquakes and subduction of the Nazca plate beneath South America. *Geology* **4,** 686–692.

Borchardt, G. A., Aruscavage, P. J., and Millard, H. T., Jr. (1972). Correlation of the Bishop ash, a Pleistocene marker bed, using instrumental neutron activation analysis. *Journal of Sedimentary Petrology* **42,** 301–306.

Clapperton, C. M., and Vera, R. (1986). The Quaternary glacial sequence in Ecuador: A reinterpretation of the work of Walter Sauer. *Journal of Quaternary Science* **1,** 45–56.

Colinvaux, P. A., Bush, M. B., Steinitz-Kannan, M., and Miller, M. C. (1997). Glacial and postglacial pollen records from the Ecuadorian Andes and Amazon. *Quaternary Research* **48,** 69–78.

Delano, J. W., Tice, S. J., Mitchell, C. E., and Goldman, D. (1994). Rhyolitic glass in Ordovician K-bentonites: A new stratigraphic tool. *Geology* **22,** 115–118.

Direccíon General de Geología y Minas. (1975). Mapa Geologico del Ecuador, Hoja 53 (Cuenca) 1:100,000: Quito.

Francis, P. (1993). "Volcanoes: A Planetary Perspective." Oxford University Press, Oxford.

Froggatt, P. C. (1992). Standardization of the chemical analysis of tephra deposits. Report of the ICCT Working Group. *Quaternary International* **13,** 93–96.

Goodman, A. Y. (1996). "Glacial Geology and Soil Catena Development on Moraines in Las Cajas National Park, Ecuador." Unpublished B.S. thesis, Union College, Schenectady, New York.

Hall, M. L., and Beate, B. (1991). El volcanismo plio-cuaternario en los Andes del Ecuador. *In* "El Paisaje Volcanico de la Sierra Ecuatoriana" (P. A. Mothes, Ed.), pp. 5–17. Corporacion Editora Nacional, Quito. [In Spanish]

Hall, M. L., and Mothes, P. A. (1994). Tefroestratigrafía holocénica de los volcanes principales del valle interandino, Ecuador. *In* "El Contexto Geológico del Espacio Físico Ecuatoriano" (R. Marocco, Ed.), pp. 47–67. Corporación Editora Nacional, Quito. [In Spanish]

Hall, M. L., and Wood, C. A. (1985). Volcano-tectonic segmentation of the northern Andes. *Geology* **13,** 203–207.

Hallett, D. J., Mathewes, R. W., and Foit, F. F., Jr. (2001). Mid-Holocene glacier peak and Mount St. Helens We tephra layers detected in lake sediments from Southern British Columbia using high resolution techniques. *Quaternary Research* **55,** 284–292.

Hunt, J. B., and Hill, P. G. (1993). Tephra geochemistry: A discussion of some persistent analytical problems. *The Holocene* **3,** 271–278.

Mothes, P. A. (1992). Lahars of Cotopaxi Volcano, Ecuador: Hazard and risk evaluation. *In* "Geohazards Natural and Man-made" (G. J. H. McCall, D. J. C. Laming, and S. C. Scott, Eds.), pp. 53–63. Chapman and Hall, London.

Mothes, P. A., and Hall, M. L. (1991). El paisaje interandino y su formación por eventos volcánicos de gran magnitud. *In* "El Paisaje Volcanico de la Sierra Ecuatoriana" (P. A. Mothes, Ed.), pp. 19–38. Corporacion Editora Nacional, Quito. [In Spanish]

Nebolini, J. C., 1996, "Geochemical Fingerprinting of Tephra Layers Preserved in Lake Cores in Las Cajas National Park, Ecuador." Unpublished B.S. thesis, Union College, Schenectady, New York.

Nielsen, C. H., and Sigurdsson, H. (1981). Quantitative methods for electron microprobe analysis of sodium in natural and synthetic glasses. *American Mineralogist* **66,** 547–552.

Rodbell, D. T., Seltzer, G. O., Abbott, M. B., Hansen, B. C. S., Goodman, A. Y., and Nebolini, J. C. (1996). Tephrochronology, sedimentology, and palynology of late glacial-Holocene lake sediment cores from southern Ecuador. *EOS Transaction* **77,** F30.

Rodbell, D. T., Seltzer, G. O., Anderson, D. M., Abbott, M. B., Enfield, D. B., and Newman, J. H. (1999). A ∼15,000 year record of El-Niño driven alluviation in southwestern Ecuador. *Science* **283,** 516–520.

Sillitoe, R. H. (1974). Tectonic segmentation of the Andes: Implications for magmatism and metallogeny. *Nature* **250,** 542–545.

Stuiver, M., Reimer, P. J., Bard, E., Beck, J. W., Burr, G. S., Hughen, K. A., Kromer, B., McCormac, F. G., van der Plicht, J., and Spurk, M. (1998). INTCAL 98 radiocarbon age calibration, 24,000–0 cal B.P. *Radiocarbon* **40,** 1041–1083.

Wright, H. E. (1991). Coring tips. *Journal of Paleolimnology* **6,** 37–49.